Coherent spin control of s-, p-, d- and f-electrons in a silicon quantum dot

R. C. C. Leon,[1,*] C. H. Yang,[1] J. C. C. Hwang,[1,†] J. Camirand Lemyre,[2] T. Tanttu,[1] W. Huang,[1] K. W. Chan,[1] K. Y. Tan,[3] F. E. Hudson,[1] K. M. Itoh,[4] A. Morello,[1] A. Laucht,[1] M. Pioro-Ladrière,[2,5] A. Saraiva,[1,‡] and A. S. Dzurak[1,§]

[1]*Centre for Quantum Computation and Communication Technology, School of Electrical Engineering and Telecommunications, The University of New South Wales, Sydney, NSW 2052, Australia.*
[2]*Institut Quantique et Département de Physique, Université de Sherbrooke, Sherbrooke, Québec J1K 2R1, Canada*
[3]*QCD Labs, COMP Centre of Excellence, Department of Applied Physics, Aalto University, 00076 Aalto, Finland*
[4]*School of Fundamental Science and Technology, Keio University, 3-14-1 Hiyoshi, Kohokuku, Yokohama 223-8522, Japan.*
[5]*Quantum Information Science Program, Canadian Institute for Advanced Research, Toronto, ON, M5G 1Z8, Canada*

Once the periodic properties of elements were unveiled, chemical bonds could be understood in terms of the valence of atoms. Ideally, this rationale would extend to quantum dots, often termed artificial atoms, and quantum computation could be performed by merely controlling the outer-shell electrons of dot-based qubits. Imperfections in the semiconductor material, including at the atomic scale, disrupt this analogy between atoms and quantum dots, so that real devices seldom display such a systematic many-electron arrangement. We demonstrate here an electrostatically-defined quantum dot that is robust to disorder, revealing a well defined shell structure. We observe four shells (31 electrons) with multiplicities given by spin and valley degrees of freedom. We explore various fillings consisting of a single valence electron – namely 1, 5, 13 and 25 electrons – as potential qubits, and we identify fillings that yield a total spin-1 on the dot. An integrated micromagnet allows us to perform electrically-driven spin resonance (EDSR). Higher shell states are shown to be more susceptible to the driving field, leading to faster Rabi rotations of the qubit. We investigate the impact of orbital excitations of the p- and d-shell electrons on single qubits as a function of the dot deformation. This allows us to tune the dot excitation spectrum and exploit it for faster qubit control. Furthermore, hotspots arising from this tunable energy level structure provide a pathway towards fast spin initialisation. The observation of spin-1 states may be exploited in the future to study symmetry-protected topological states in antiferromagnetic spin chains and their application to quantum computing.

8 / 11 /2019

FAM

Leon Camenzind

Motivation

Orbitals play major role in performance & operation of semiconductor spin qubits

Spin relaxation (in GaAs)

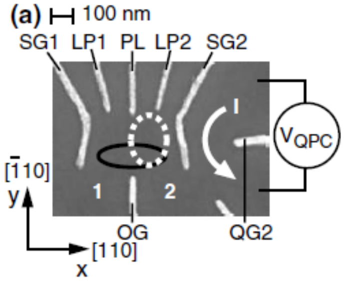

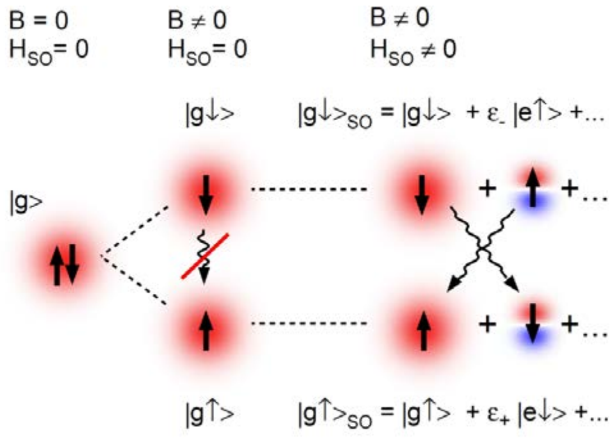

$$W = T_1^{-1} \propto \frac{B^5}{\lambda_{SO}^2 \cdot E_{orb}^4}$$

$$E_{orb} = \frac{\hbar}{m^* \cdot l_{orb}^2}$$

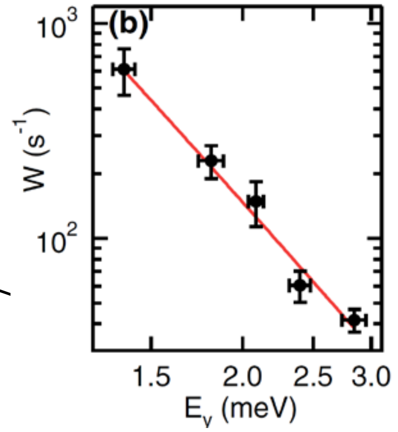

Amasha *et al.*, PRL **100** (2008).

Qubit drive (Rabi oscillations)

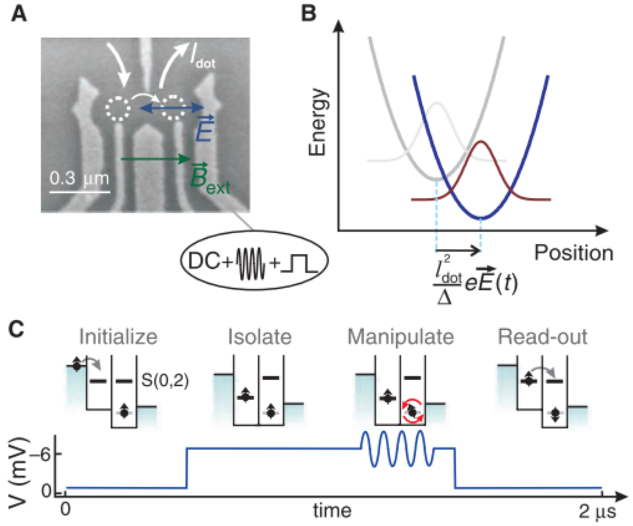

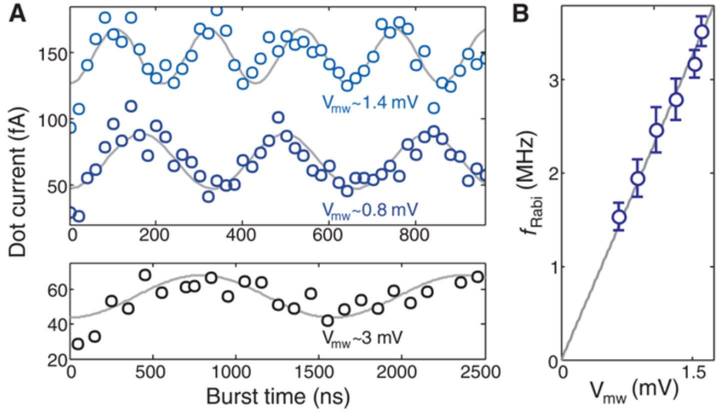

$$f_{Rabi} \propto g\,\mu_B \,\frac{|E(t)|}{E_{orb}^2}\left(|b_{SL}| - \frac{2|B_0|}{l_{so}}\right) / \, 2h$$

micromagnets

SOI

Pioro-Ladrière *et al. Nat. Phys.* 4 (2008)

Nowack *et al.*, *Science* 318 (2007)

Device & charge stability

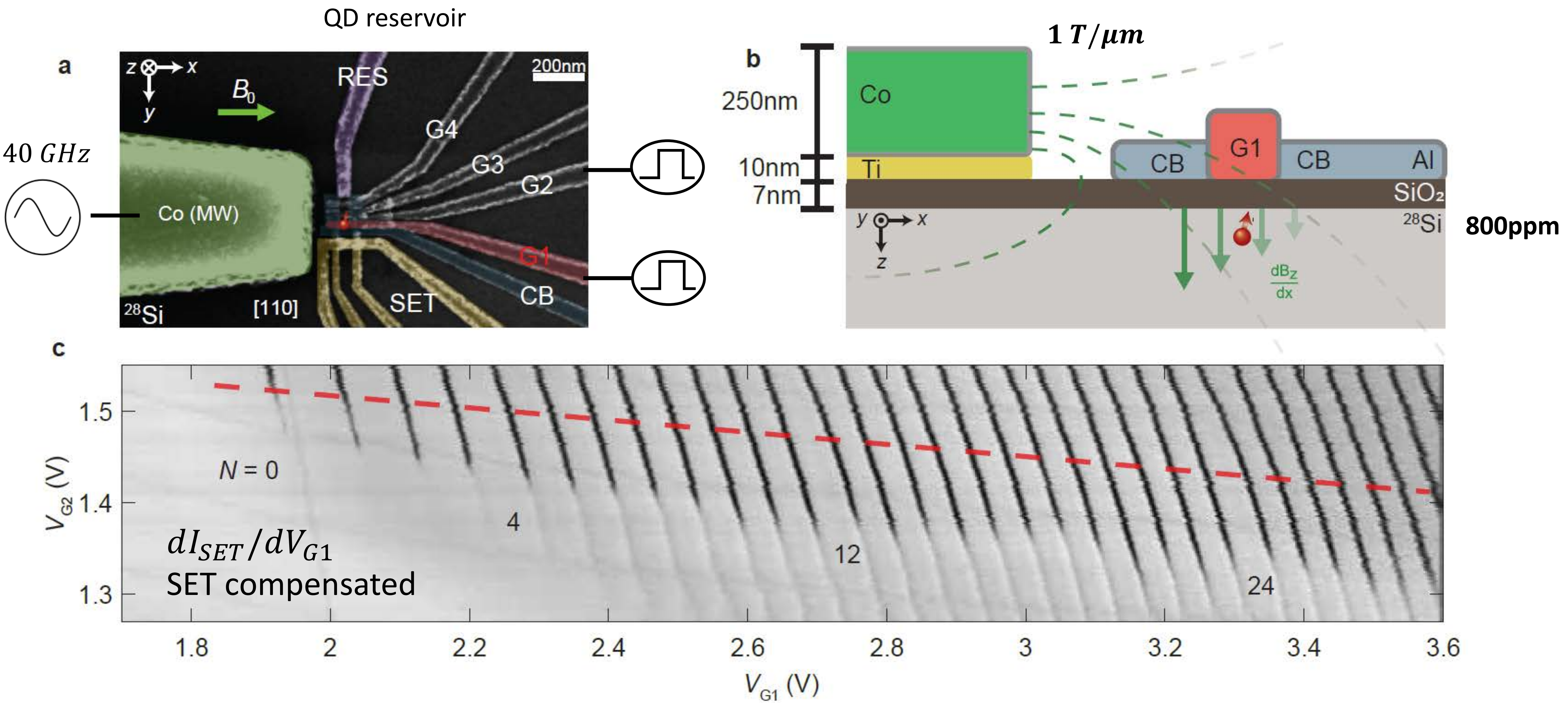

Shell filling: «Magic numbers»

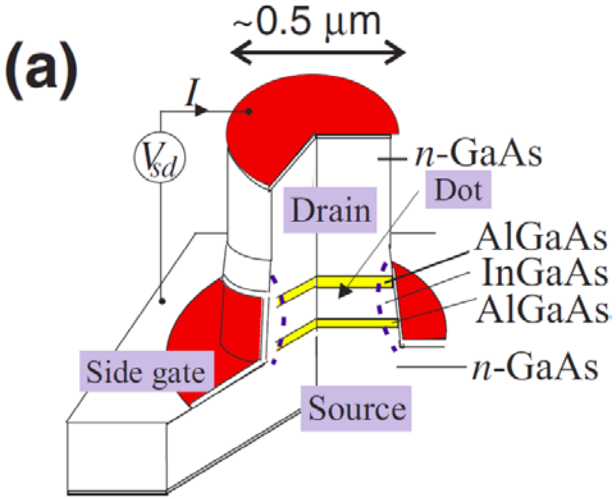

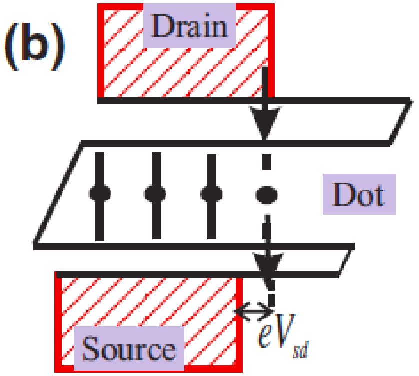

Charging energy $\boldsymbol{E_c}$

$C \sim 8\epsilon_r\epsilon_0 r$ (Disk)

$E_C = e^2/C$

Orbitals (isotropic 2D-dot)

$$E_{nl} = (2n + |l| + 1)\hbar\left(\frac{1}{4}\omega_c^2 + \omega_0^2\right)^{1/2} - \frac{1}{2}l\,\hbar\omega_c$$

$n = 0,\ 1,\ 2,..$ (radial quantum number)

$l = \ 0, \pm 1, \pm 2$ (angular momentum)

$$\boldsymbol{E_{add} = E_C + (E_{orb})}$$

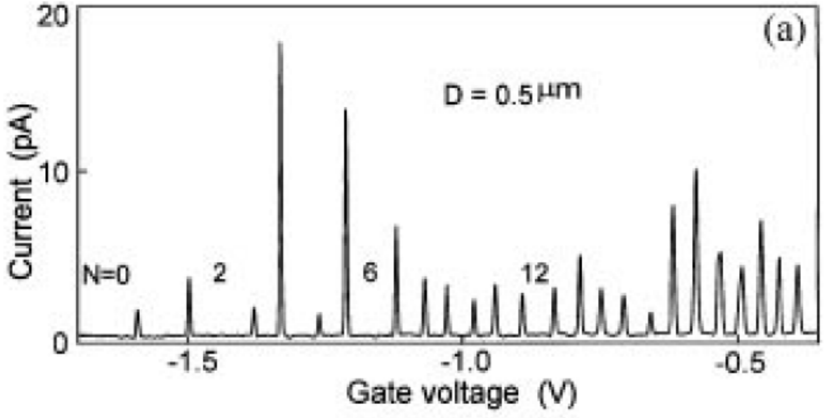

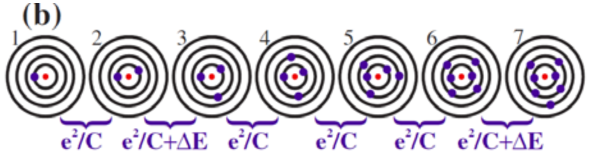

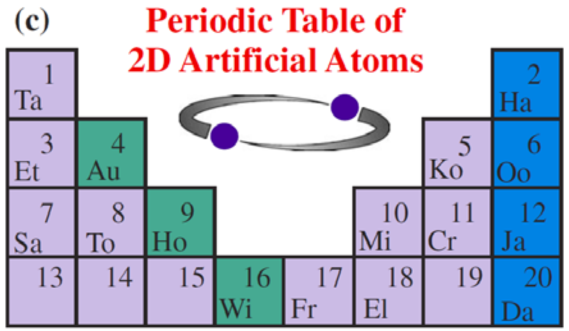

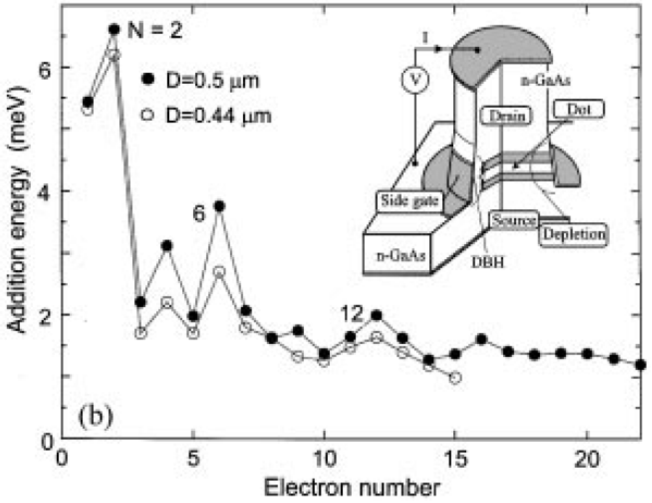

Tarucha *et al.*, *PRL* 77 (1996)

Kouwenhoven, Austing, Tarucha, *Rep. on Prog. in Phys.*, 64 (2001)

Magic numbers with valley degeneracy

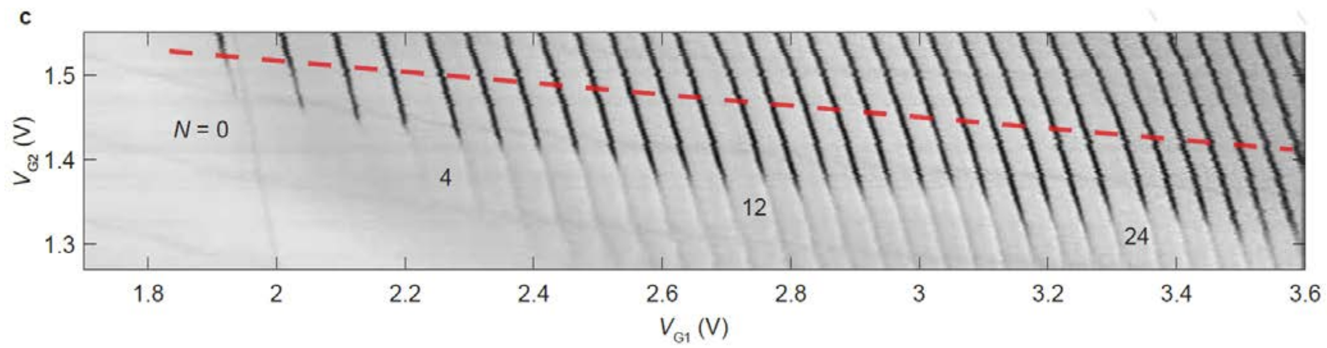

+ inluding valley degeneracy in silicon (2x)

magic numbers:

2, 6, 12 → 4, 12, 24

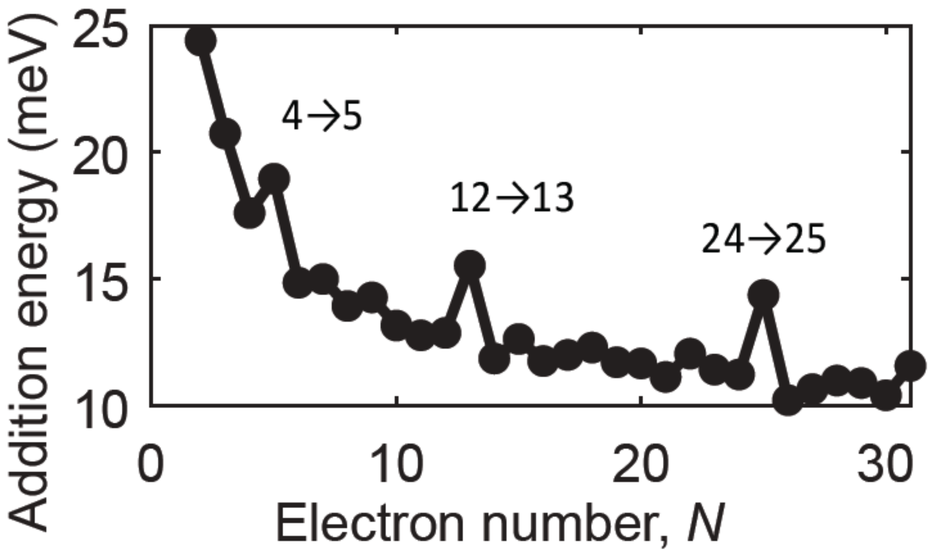

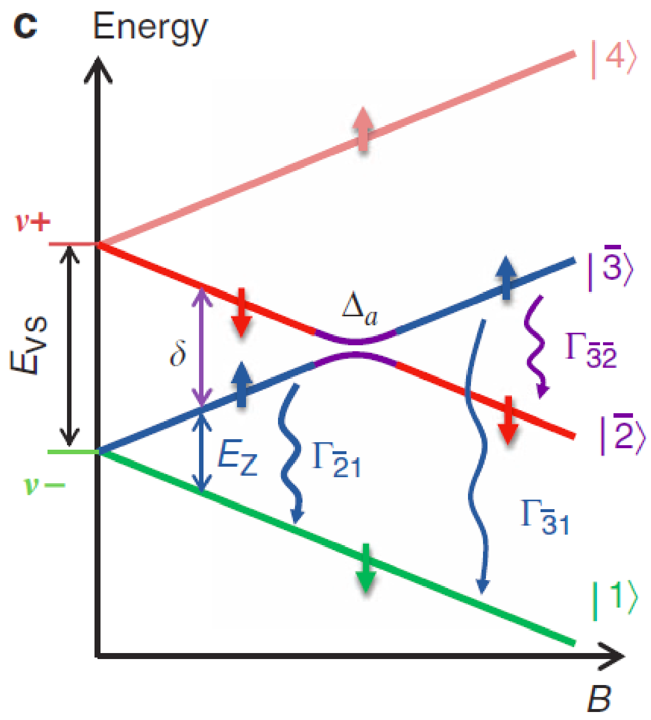

Magnetospectroscopy

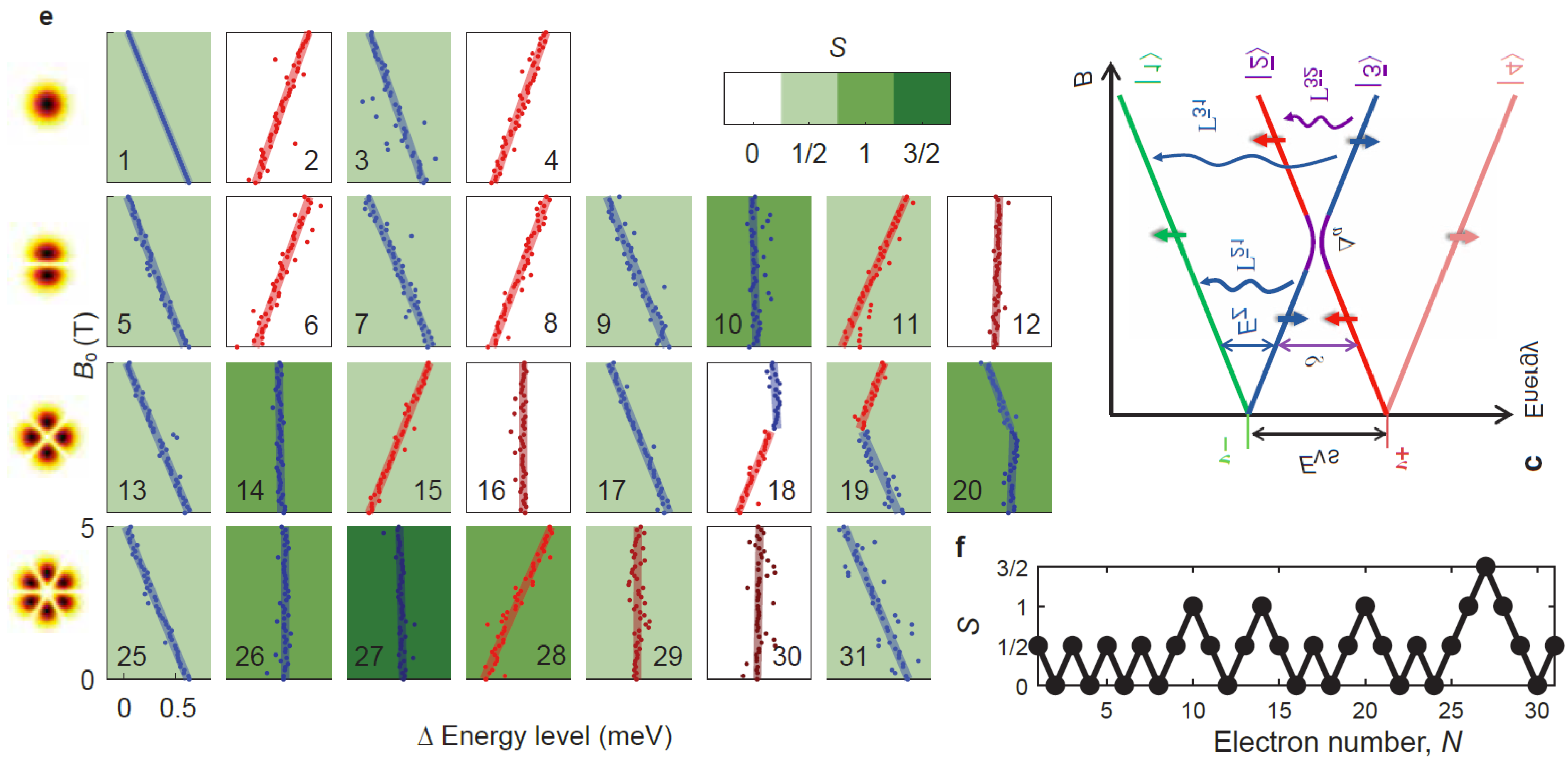

see also Liles *et al.,* Nature Comms. 9, 3255 (2018) [holes] and Yang et al, Nat. Comm. 3069 (2013) [electrons]

Driving and read-out of the qubit

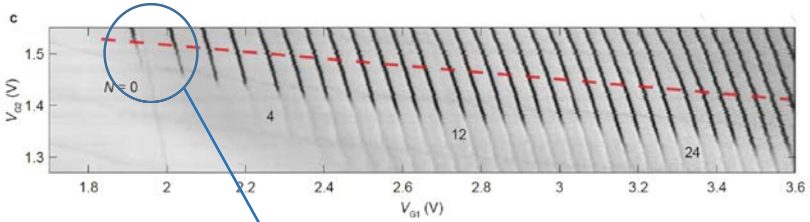

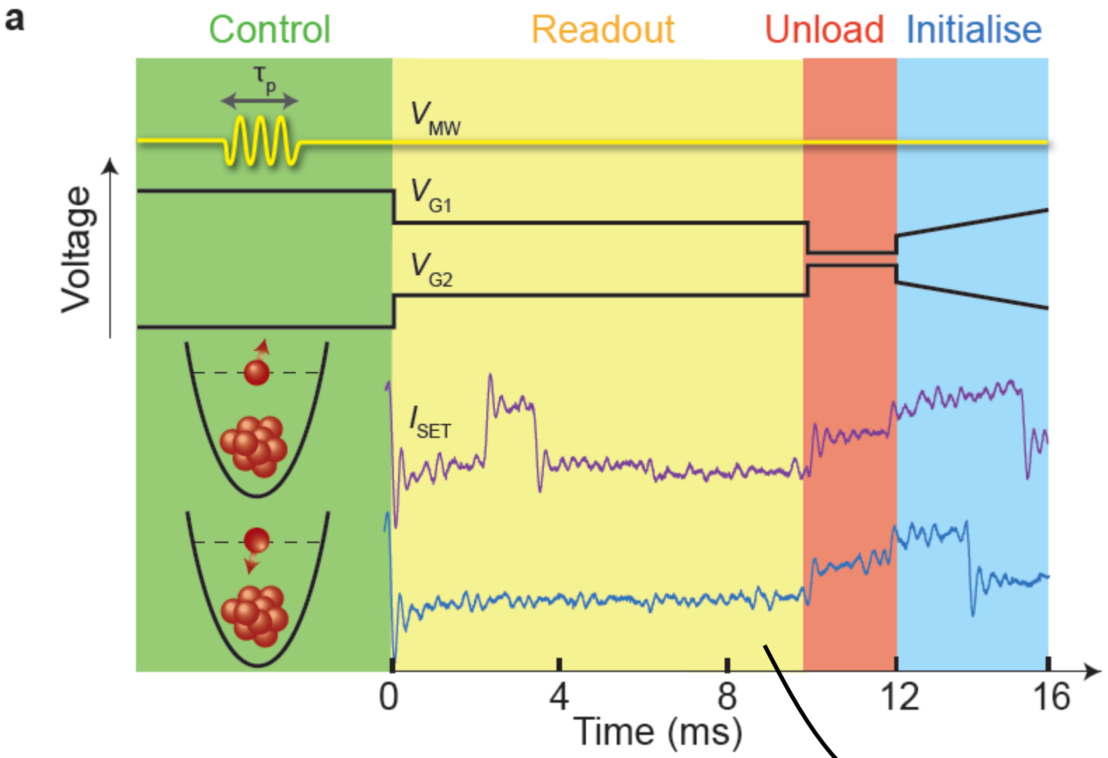

Qubit drive

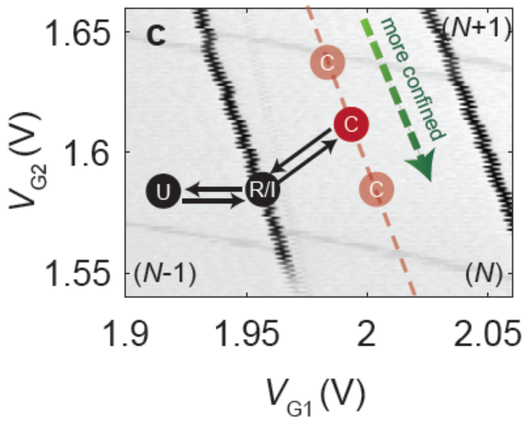

spin relaxation

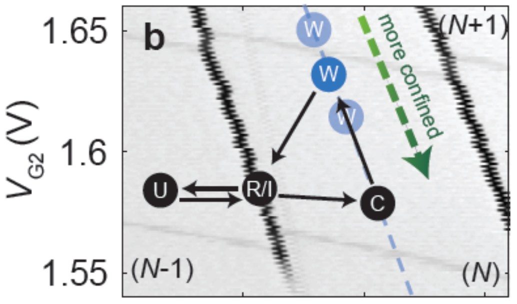

π pulse @ C

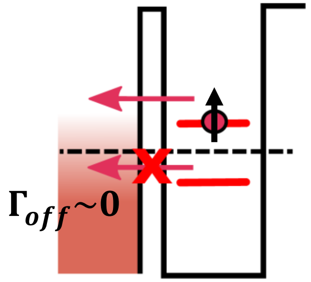

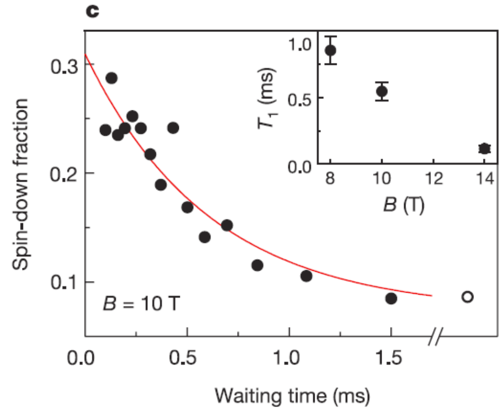

spin to charge conversion

Elzerman *et al.*, *Nature*, 430 (2004).

Coherent spin control

Larmor frequency:	$f_0 = 41.829$ GHz	$f_0 = 41.879$ GHz	$f_0 = 41.827$ GHz

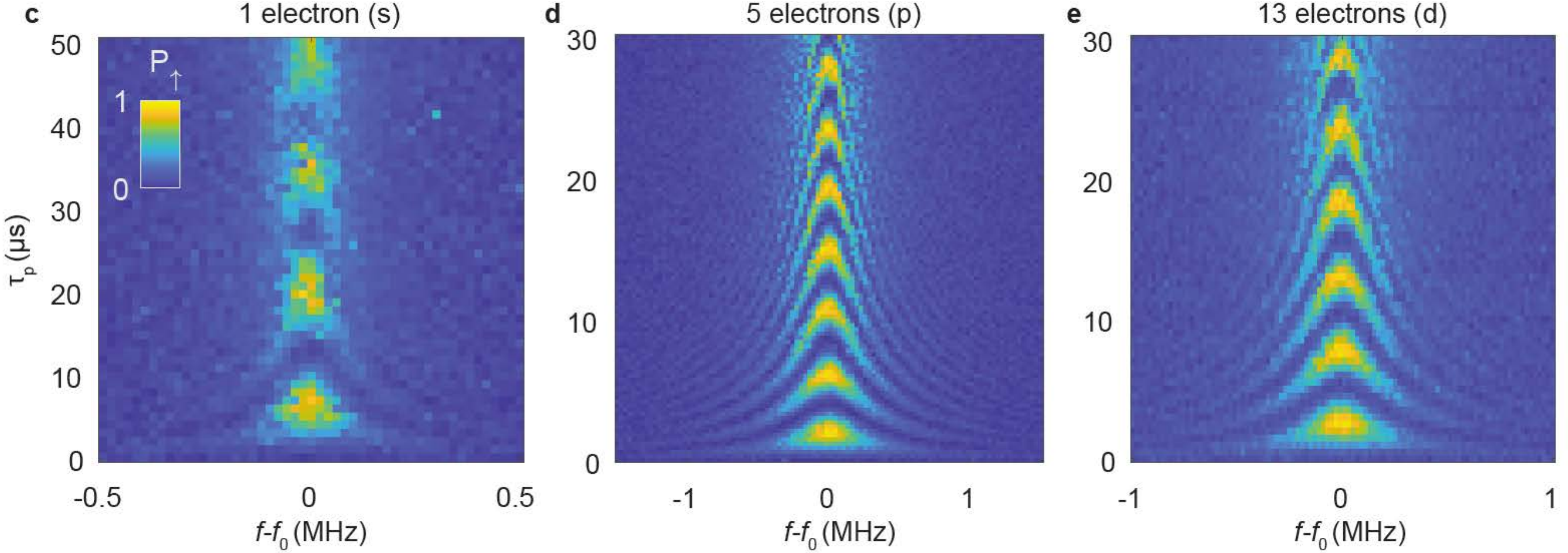

$\boldsymbol{f_{Rabi}}$	$\sim 10kHz$	$\sim 200\ kHz$	$\sim 200\ kHz$
$\boldsymbol{T_2^*}$	$\sim 18\mu s$	$16\mu s$	$7\mu s$

$$f_{Rabi} \propto g\,\mu_B\,\frac{|E(t)|}{E_{orb}^2}\left(|b_{SL}| - \frac{2|B_0|}{l_{so}}\right) / \,2h$$

Decoherence T_2^*: electric noise + $|b_{SL}|$

Micromagnet-ESR

Pioro-Ladrière *et al. Nat. Phys.*, 4 (2008)

EDSR: SOI (very weak interface Dresselhaus)

Nowack *et al.*, *Science* 318 (2007)

Quality factor for different shells

$$f_{Rabi} \propto g\,\mu_B \frac{|E(t)|}{E_{orb}^2}\left(|b_{SL}| - \frac{2|B_0|}{l_{so}}\right) / 2h$$

$$Q = T_2^{Rabi}/T_\pi$$

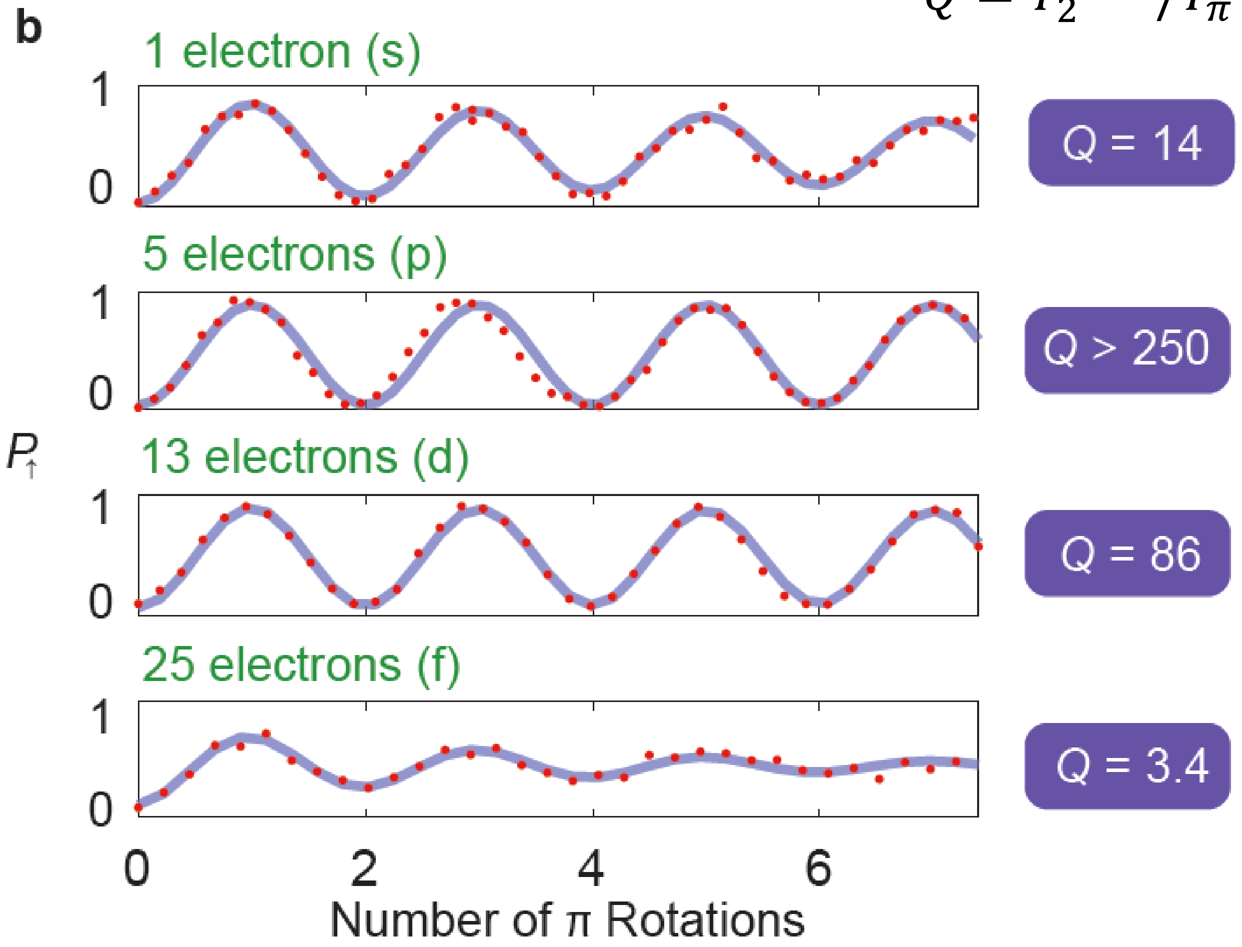

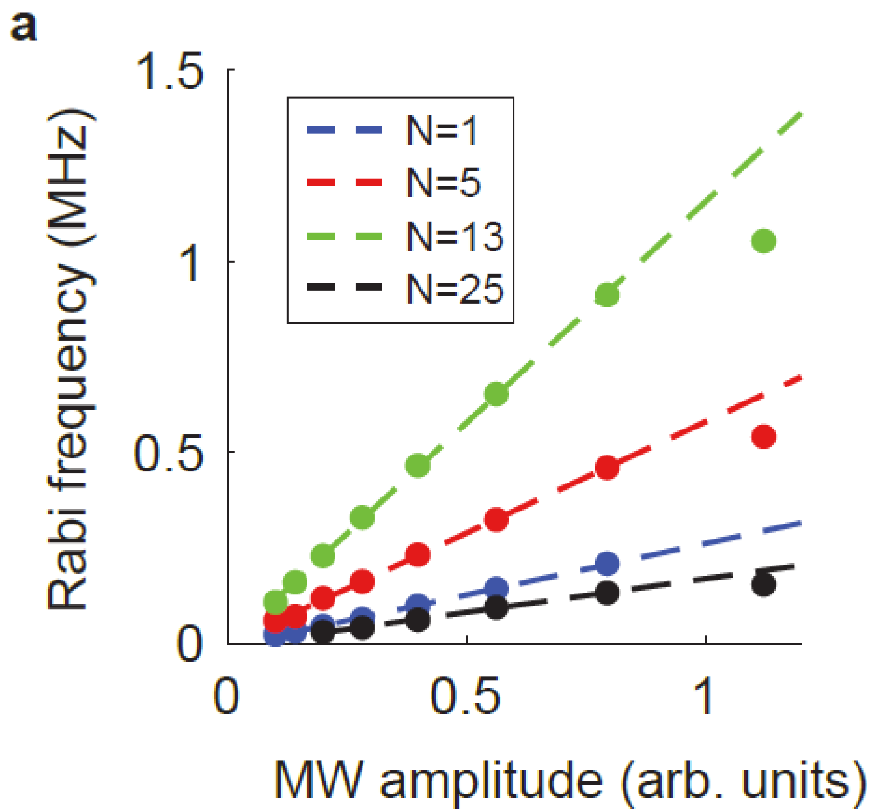

Gate fidelities: Randomized benchmaring

Idea: obtain gate fidelities by removing read-out infidelities out of the sequence

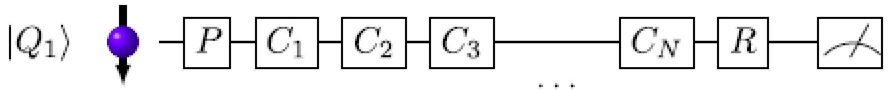

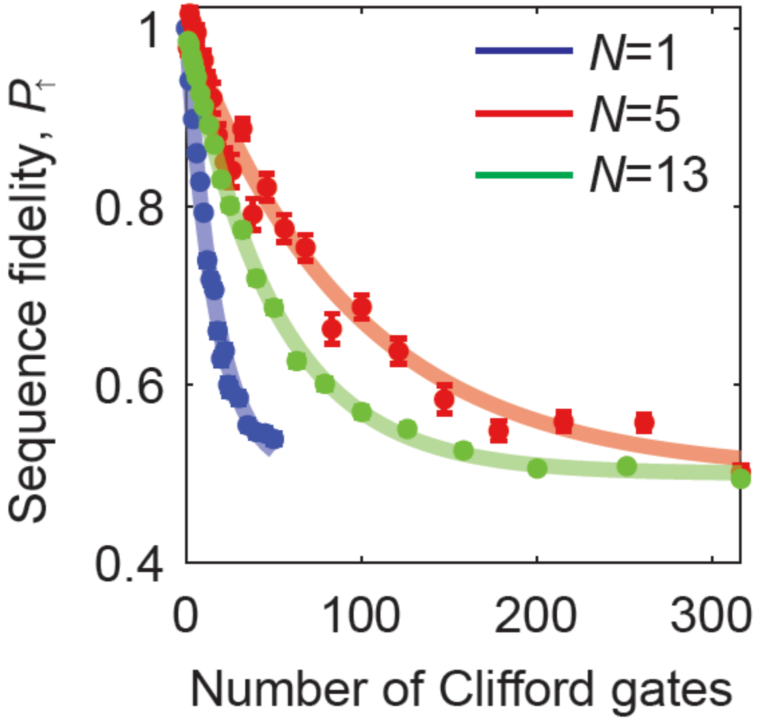

- Create random sequence of Clifford gates $\{I, \pm X, \pm X^2, \pm Y, \pm Y^2\}$ of length m
- at the end: refocus pulse
- Apply sequence to either $|\uparrow\rangle$ and $|\downarrow\rangle$ $\rightarrow$ $P_{|1\rangle}$ resp. $P'_{|1\rangle}$

$$P'_{|1\rangle} - P_{|1\rangle} = ap^m$$

- Average Clifford-gate fidelities: $F_C = 1 - (1 - p)/2$

shell	electrons	gate fidelities
s	1	98.5
p	5	99.7
d	13	99.5

similar T_2 but much faster gates → higher fidelity

Confinement dependence

$f_0 \sim 41GHz$ increase in E_{orb}

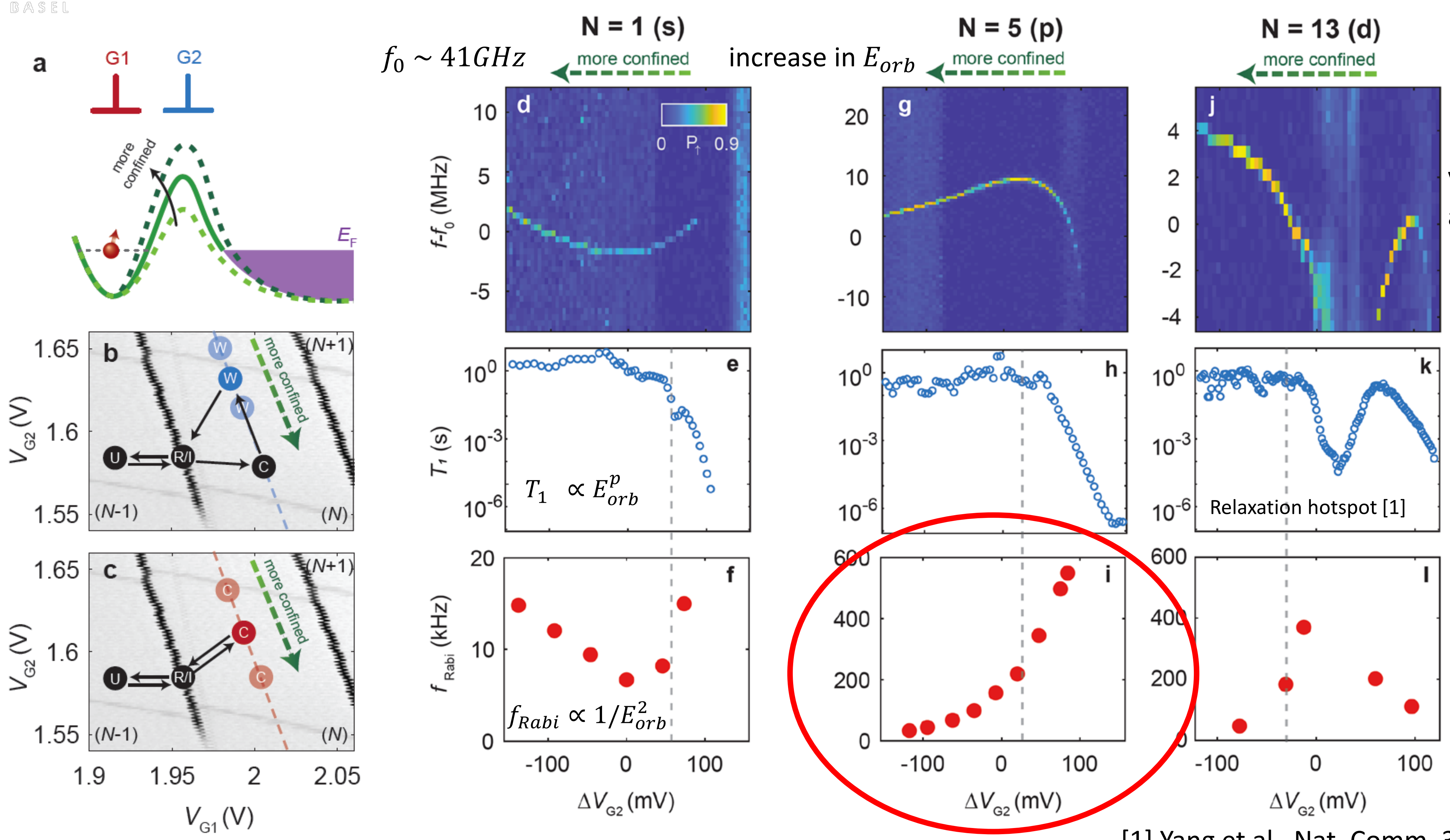

Stark Shift

Variations of g-factor and/or micromagnet field

Orbital effects

Excited orb. state or valley state near Zeeman excitation

Orbital effects

f_{rabi} correlates with df/dV_{G2}

$f_{Rabi} \propto \frac{|b_{SL}|}{E_{orb}^2}$

[1] Yang et al, Nat. Comm. 3069 (2013)

But what about T2 and Q?

5 electron configuration

more confined ←

T_2 sweetspot (*):
less successible to charge noise: @ $df/dV_g \sim 0$

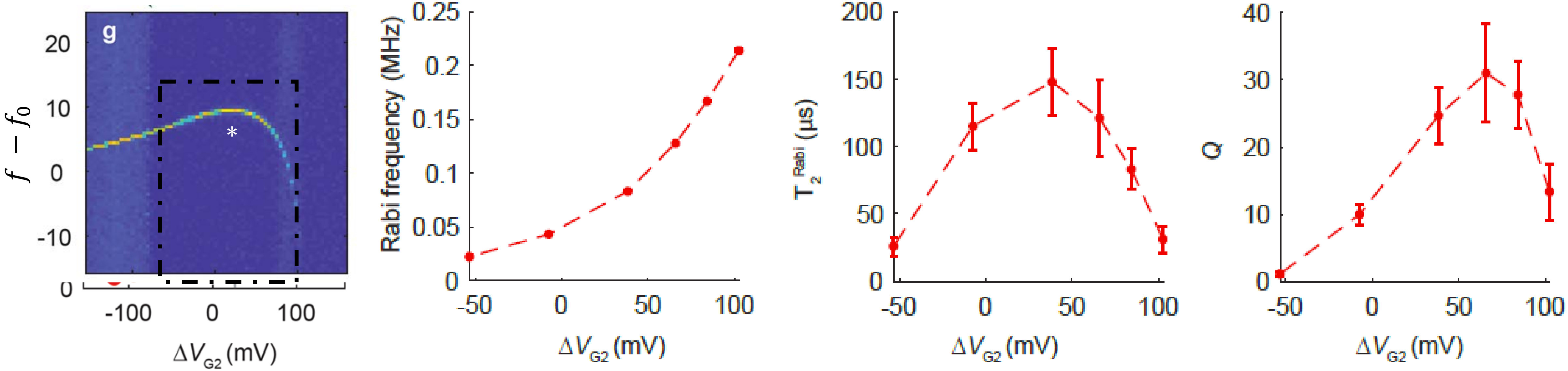

Data from the lab
(Ge/Si NW qubit):

much stronger gate tuneability

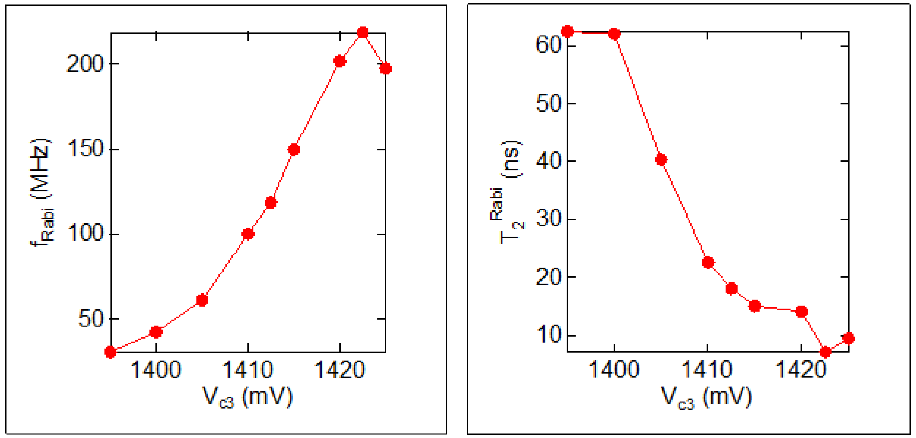

orbital effect or indication of direct Rashba SOI?

more confined →

Conclusions

BASEL

- Qubit operation hotspot in p-shell:
  - faster driving (orbital energy / size)
  - same T_2 as for s-shell
    → increase in **quality factor and gate fidelities**

- Electrical tunability of Qubit parameters...
  - Stark shift (weak)
  - T_1
  - T_2
  - f_{Rabi}

... due to orbital and valley effects..

Thank you for your attention

Appendix

Coherent control of other electron occupancies

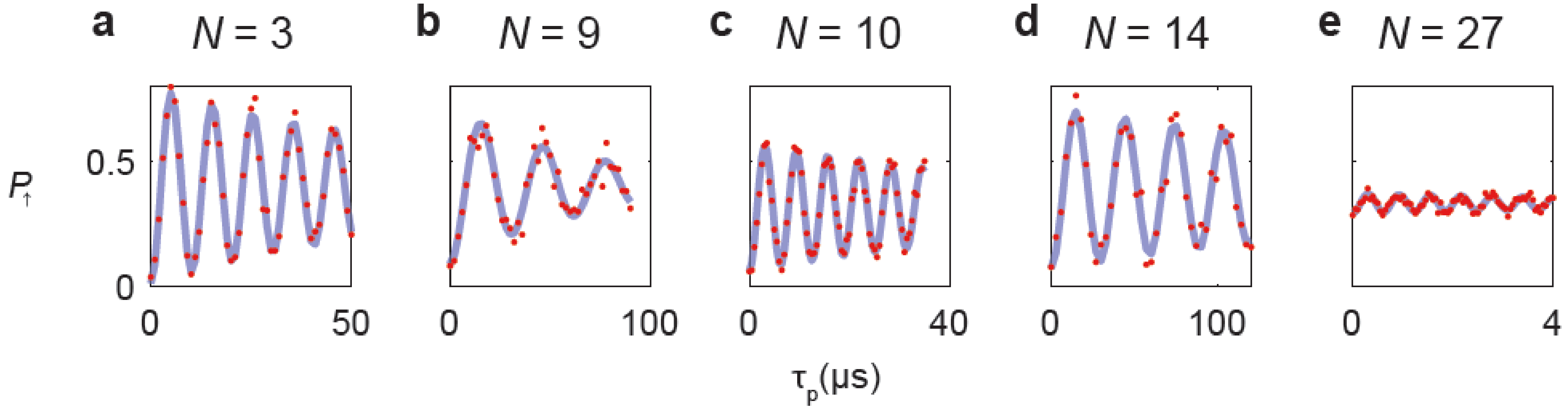

Extended Figure 2 |Coherent control at various electron occupancies. Rabi oscillations at different electron numbers N inside the a single quantum dot. (a) $N = 3$ (b) $N = 9$ (c) $N = 10$ (d) $N = 14$ (e) $N = 27$. Note that from Fig. 1f, N =10 and 14 electrons have total spin states $S = 1$, while N =27 electrons has $S = \frac{3}{2}$.

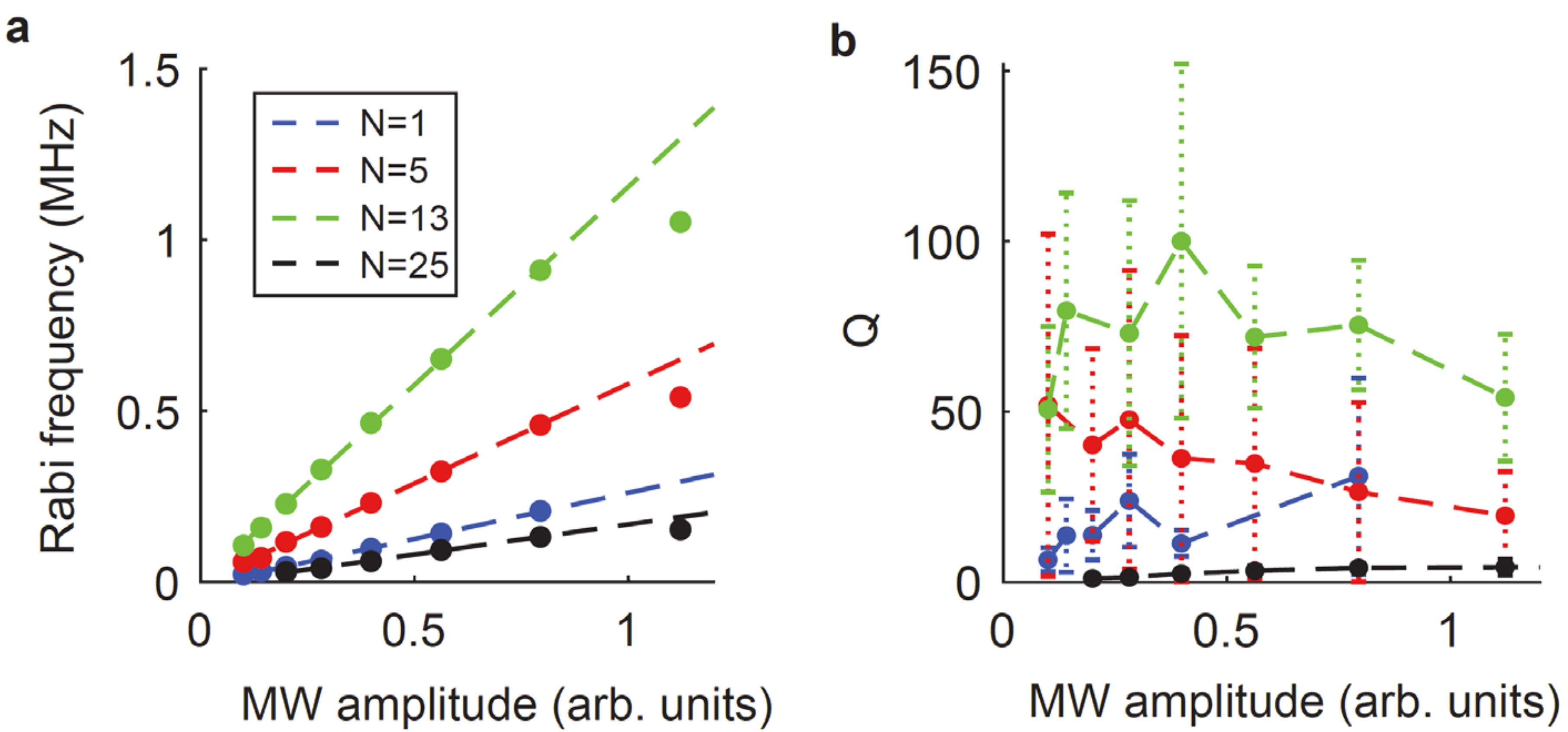
a
Rabi frequency (MHz)
1.5
1
0.5
0
N=1
N=5
N=13
N=25
0
0.5
1
MW amplitude (arb. units)
b
Q
150
100
50
0
0
0.5
1
MW amplitude (arb. units)

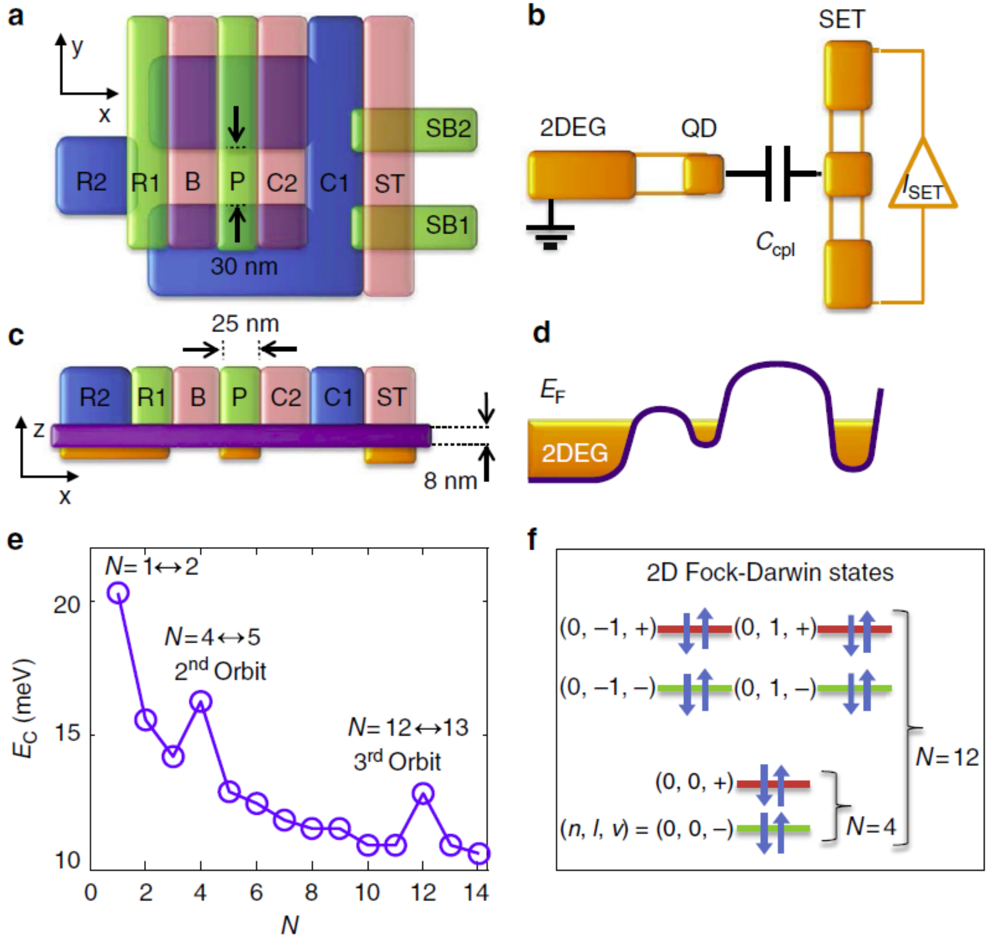

a
y
x
SB2
R2
R1
B
P
C2
C1
ST
SB1
30 nm
b
SET
2DEG
QD
I_SET
C_cpl
c
25 nm
z
x
8 nm
d
E_F
2DEG
e
N=1↔2
N=4↔5
2nd Orbit
N=12↔13
3rd Orbit
E_C (meV)
N
f
2D Fock-Darwin states
(0, −1, +)
(0, 1, +)
(0, −1, −)
(0, 1, −)
(0, 0, +)
(n, l, v) = (0, 0, −)
N=4
N=12

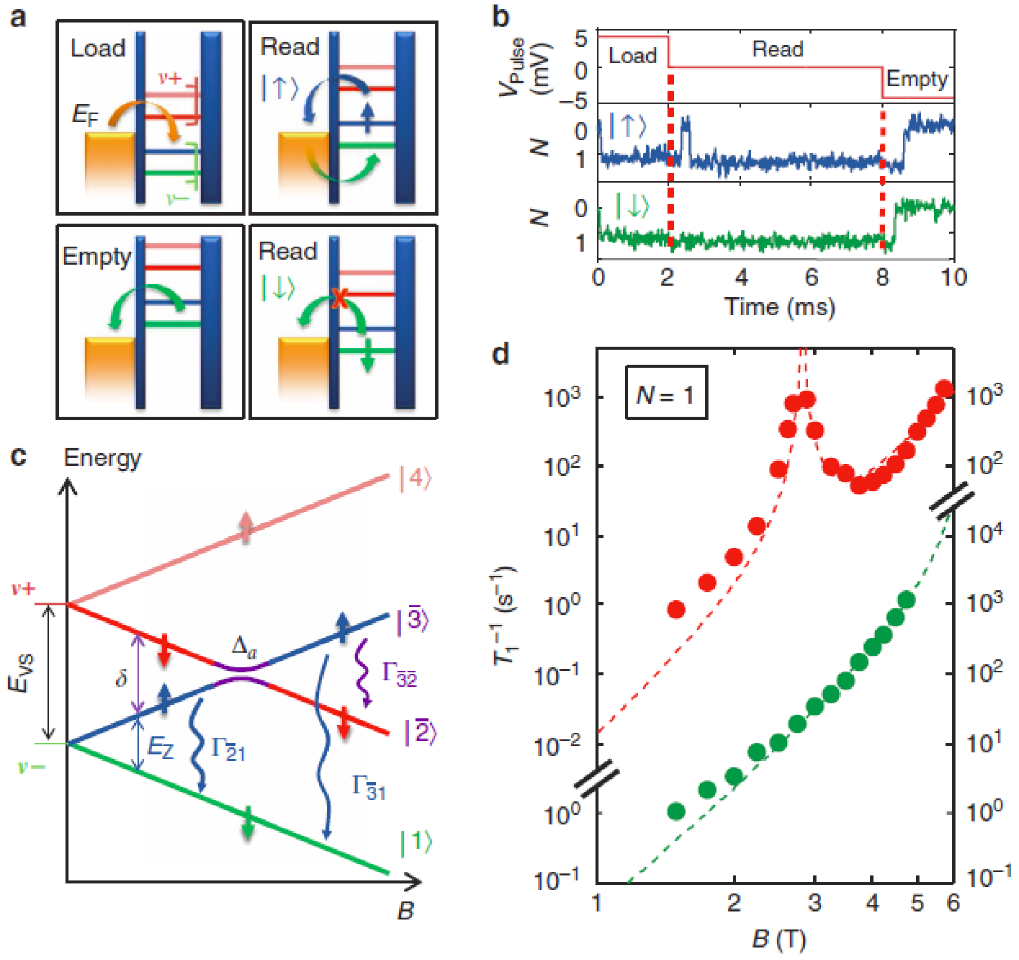

a
Load
Read
|↑⟩
E_F
v+
v−
Empty
Read
|↓⟩
b
V_Pulse (mV)
Load
Read
Empty
N
|↑⟩
|↓⟩
Time (ms)
c
Energy
|4⟩
|3̄⟩
|2̄⟩
|1⟩
v+
v−
E_VS
δ
Δ_a
E_Z
Γ_21
Γ_32
Γ_31
B
d
N = 1
T_1^−1 (s^−1)
B (T)

Liles et al., Nat. Commun.

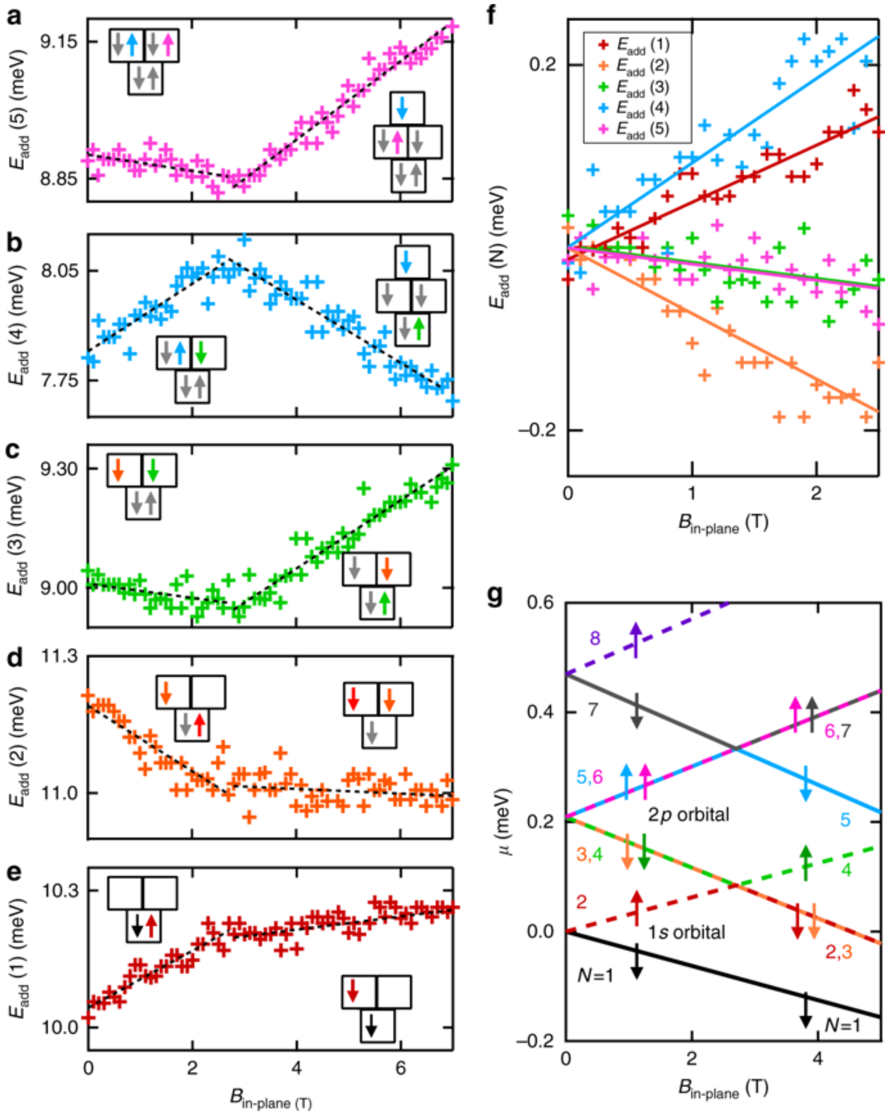

Spin relaxation due to SOI mediated coupling to phonons

BASEL

Piezoelectric electron-phonon interaction:

$$U_{ph} \propto \omega^{-\frac{1}{2}} \cdot e^{i(\vec{q}\vec{r}-\omega t)} \rightarrow E_\omega \propto \left|-\nabla U_{ph}\right| \propto q\omega^{-\frac{1}{2}} \rightarrow q^{\frac{1}{2}}$$

$$H_{so} \propto \frac{1}{\hbar\omega_0 + \Delta} - \frac{1}{\hbar\omega_0 \ - \Delta} \ \ using\ \Delta \ll \hbar\omega_0 \rightarrow H_{so} \propto \frac{\Delta}{(\hbar\omega_0)^2}$$

First order spin flip transition matrix element:

$$M \approx {}_{eff}\langle g \downarrow \left|U_{ph}\right| g \uparrow\rangle_{eff} \propto q^{\frac{1}{2}} \cdot H_{so} \cdot \Delta \propto q^{\frac{1}{2}} \cdot \Delta \cdot (\hbar\omega_0)^{-2}$$

Using Fermis golden Rule:

$$\mathrm{W} = \frac{2\pi}{\hbar^2} |M|^2 D_{ph}(q) \longleftarrow D_{ph}(q) \propto q^2$$

Spin relaxation rate for $\boldsymbol{q} \propto \boldsymbol{\Delta}$ **(energy matching)**

$$W \propto \left|q^{\frac{1}{2}}\Delta\ (\hbar\omega_0)^{-2}\right|^2 q^2 = \frac{\Delta^5}{(\hbar\omega_0)^4}$$

Δ^5 ← 3x phonons, 2x SOI

$(\hbar\omega_0)^4$ ← 4x SOI

$$T_1^{-1} = W = A \cdot \frac{B^5}{\lambda_{SO}^2 \cdot (\hbar\boldsymbol{\omega_0})^4}$$

From Golovach *et al.*, PRL 93 (2004) $\boldsymbol{A} \approx 33\ s^{-1}\mathrm{mev}^4\mu m^2/T^5$